ICAS 2016
30th Congress of the International Council of the Aeronautical Sciences
DCC, Daejeon, Korea ; September 25-30, 2016

STOCHASTIC TRANSONIC AERODYNAMICS ANALYSIS

Xiaojing Wu, WeiweiZhang*
*** School of Aeronautics, Northwestern Polytechnical University**

Keywords: *uncertainty quantification, sensitivity analysis, non-intrusive polynomial chaos, principal component analysis, transonic aerodynamics*

Abstract

Uncertainty quantification is applied to compute its impact on the aerodynamic characteristics. In addition, the contribution of each uncertainty variable to aerodynamic characteristics need to be computed by the uncertainty sensitivity analysis. In this paper, the Sobol's analysis is used to uncertainty sensitivity analysis and a non-intrusive polynomial chaos method is used to uncertainty quantification and Sobol's analysis. By uncertainty quantification, we can learn that the flow characteristics of shock wave and boundary-layer separation is sensitive to the geometric uncertainty in transonic region, which is the main reason that transonic drag is sensitive to the geometric uncertainty. The sensitivity analysis shows that the model can be simplified by eliminate unimportant geometric modes for UQ. Moreover, we can learn which typical geometric modes is important to transonic aerodynamics.

1 Introduction

With the development of computer technology, computational fluid dynamics(CFD) technology has been widely used to solve problems in aerodynamic mechanics. The traditional CFD simulation is deterministic. But in reality, with the increasing complexity of the fluid problem, a variety of uncertainties are inevitable in CFD simulation, leading to the mismatch between the CFD simulation results and the actual results[1-2].The sources and classifications of uncertainty in CFD were described in reference [3-4]. Several uncertainty quantification (UQ) strategies have been used in CFD, including Monte Carlo simulation(MCS), sensitivity analysis (SA), moment methods and polynomial chaos expansions (PCE) in reference [5]. Recently, PCE has been widely applied to UQ of fluid problems. PCE methods can be divided into intrusive and nonintrusive methods according to the coupling ways with CFD solvers. In general, an intrusive approach calculates the unknown polynomial coefficients by projecting the resulting equations into basis functions for different modes, and it requires to modify the CFD codes, which may be difficult and time-consuming for complex problems such as N-S simulation. Mathelin[6] used the intrusive PCE to research the quasi one-dimensional duct flow uncertainty propagation problems. To overcome the shortcomings of intrusive polynomial chaos, non-intrusive polynomial chaos (NIPC) has been developed. CFD is regarded as a black box model without changing the CFD program code in the non-intrusive methods. UQ based on PCE and its applications in fluid mechanics were comprehensively reviewed in Ref. [7-8].

In addition to UQ, global sensitivity analysis (GSA) plays an important role in quantifying the relative importance of each uncertainty source. By means of this technique, uncertainties can be systemically studied to measure their effects on the system outputs, so as to screen out the uncertainties with negligible contributions to simplify the problem. A comprehensive review of uncertainty sensitivity analysis can be found in Ref.[9]. The variance-based method, also called Sobol's analysis [10-11], is one of the most popular practices in many disciplines. They measure the relative importance of one input variable by the partial variance of the model output explained by this variable. Bruno [12] introduced PCE to build surrogate models that allow one to compute the

Sobol's indices analytically as a post-processing of PCE coefficients.

Most research on UQ studies the flight condition parameter uncertainty based on NIPC methods. Loeven[13] conducted a subsonic aerodynamic analysis around a NACA0012 airfoil with an uncertain free stream velocity using a commercial flow solver. From their study, an uncertain free stream velocity leads to the highest variation in pressure on the upper surface near the leading edge. Simon[14] focused on the transonic stochastic response of two-dimensional airfoil to parameter uncertainty (*Ma* and α) using gPC. Two kinds of non-linearities are critical to transonic aerodynamics in their study: the leeward shock movement characteristics and boundary-layer separation on the aft part of airfoil downstream the shock. Chassaing[15] conducted a stochastic investigation of flows about naca0012 airfoil at transonic speeds. Hosder[16] conducted a uncertainty and sensitivity analysis for reentry flows with inherent and model-form uncertainties. However, rare research can be found on stochastic aerodynamics analysis considering geometric uncertainty. The geometric uncertainty on aerodynamic surfaces resulting from manufacturing errors has significant effect on the aerodynamic performance.

In this paper, The stochastic PCE model is built to conduct UQ and SA of transonic aerodynamics. The paper is structured as follows. Section 2 introduce UQ and the variance based GSA (Sobol's analysis). In section 3, two methods, including MCS and PCE, are introduced to UQ and GSA in detail. In section 4, UQ and GSA of transonic aerodynamics are conducted. Section 5 outlines several useful conclusions

2 Uncertainty quantification and global sensitivity analysis

The aim of UQ is to compute the input parameter influence on the model's output quantitatively. The uncertainty of inputs may be expressed in a number of ways, for example, interval bounds or probability density functions. In this paper, we quantify the uncertainty by the probabilistic analysis, and focus on the robustness (mean and variance) of outputs. The mean and variance are shown by Eq. (1) and Eq. (2).

$$E_Y = E[f(\mathbf{x})] = \int_{-\infty}^{+\infty} f(\mathbf{x}) p_{\mathbf{x}}(\mathbf{x}) \quad (1)$$

$$V_Y = E[(f(\mathbf{x}) - \mu_x)^2] = \int_{-\infty}^{+\infty} [f(\mathbf{x}) - \mu_f]^2 p_{\mathbf{x}}(\mathbf{x}) \mathbf{dx} \quad (2)$$

Although UQ can identify that the uncertainty of input variables to output variables, it cannot gain the contribution of each uncertainty. In this case, SA is applied to study how uncertainty of the output of a model can be apportioned to different sources of uncertainty in the model input. The alternative uncertainty sensitivity analysis is GSA. The main goal of GSA is to demonstrate the relative importance of each input uncertainty among the overall uncertainty in the output. It is often useful to rank the contribution of each uncertainty to the overall uncertainty in the output. A detailed review of a variety of GSA methods can be found in Ref. [15]. In the current study, a variance-based global sensitivity method is used to accomplish this task. The method is based on the Sobol's variance decomposition, by which the f-function can be uniquely decomposed into 2^n functional terms of increasing dimensions

$$Y = f_0 + \sum_i f_i + \sum_i \sum_{j>i} f_{ij} + \ldots + f_{12\ldots k} \quad (3)$$

where $f_0 = E(Y), f_i = V(E(Y|X_i)) - g_0, f_{ij} = V(E(Y|X_i, X_j)) - f_i - f_j - f_0$. Taking variance is added to both sides of Eq.(3), then we can obtain below equation:

$$V(Y) = \sum_i V_i + \sum_i \sum_{j>i} V_{ij} + \cdots + V_{12\cdots k} \quad (4)$$

The first order partial variance V_i can be regarded as the average reduction of model output variance resulting from fixed X_i, that is, V_i measures the individual contribution of X_i to the total variance $V(Y)$. The larger V_i is, the more reduction of output variance can be obtained by reducing the uncertainty of X_i. The second order partial variance V_{ij} quantifies the interaction effect between X_i and X_j. Similar interpretations can be given to the higher order partial variances. Both sides of Eq. (4) divided by V_Y, we obtain:

$$S_{i_1,\ldots i_s} = V_{i_1,\ldots i_s} / V \quad (5)$$

$$\sum_i S_i + \sum_i \sum_j S_{ij} + \sum_i \sum_{j>i} \sum_{l>j} S_{ijl} + \ldots + S_{123\ldots k} = 1 \quad (6)$$

$S_{i_1\ldots i_s}$ are Sobol's indices, which measure the relative contribution to the total variance. S_i is the main sensitivity index. $S_{ij}, S_{ijl}, \ldots, S_{123\ldots k}$ measure the interaction effects.

$$S_i = \frac{V[E(Y|X_i)]}{V_Y} \tag{7}$$

Another commonly used measurement is the total partial variance V_{Ti}, which is defined as the summation of all terms in Eq.(4) with subscripts including i. In other words, V_{Ti} incorporates both the individual effect of X_i and its interaction effects with all the other input variables.

$$S_{Ti} = \frac{V_{Ti}}{V(Y)} = \frac{V(Y) - V(E(Y|\mathbf{X}_{\sim i}))}{V(Y)} = \frac{E(V(Y|\mathbf{X}_{\sim i}))}{V(Y)} \tag{8}$$

Usually S_i is used to select important variables, while S_{Ti} is more suitable to screen non-influential variables.

3 The non-intrusive polynomial chaos method for uncertainty quantification and global sensitivity analysis

The PCE is a stochastic method based on the spectral representation of uncertainty. According to the spectral representation, the random function can be decomposed into deterministic and stochastic components. A random variable X can be represented by the Eq.(9):

$$X(\mathbf{x},\xi) = \sum_{j=0}^{\infty} \alpha_j(\mathbf{x})\Psi_j(\xi) \approx \sum_{j=0}^{P} \alpha_j(\mathbf{x})\Psi_j(\xi) \tag{9}$$

where $\alpha_j(\mathbf{x})$ is the deterministic component and $\Psi_j(\xi)$ is the random basis function corresponding to the j-th mode. From Eq. (9), the random variable X is the function of deterministic independent variable vector x and the n-dimensional standard random variable vector $\xi = (\xi_1, \xi_2, \cdots, \xi_n)$. The polynomial chaos expansion given by Eq. (9) contains an infinite number of terms. In a practical computational context, the terms of PCE can be truncated by both order p and dimension n. The number of terms is finite, which is given by Eq.(10):

$$N_t = P + 1 = \frac{(n+p)!}{n!\,p!} \tag{10}$$

where n is the number of random dimensions and p is the order of polynomial chaos. When the input uncertainty obeys Gauss distribution, the basis function is the multi-dimensional Hermite polynomial.

There are two ways to solve the coefficients of Eq. (9): intrusive and non-intrusive methods. The intrusive method computes the unknown polynomial coefficients by projecting the resulting equations into basis functions for different modes. It requires the modification of the deterministic code, which may be difficult, expensive, and time-consuming for complex computational problems such as complex N-S equations. Alternatively, the non-intrusive method treats the CFD as a black box without changing the program code when propagating uncertainty. Now, we pay close attention to how to solve the coefficients in non-intrusive methods. There are two method: projection method and regression method.

The main idea of projection method is to use Galerkin projection to solve coefficients. Eq. (9) can be transformed to Eq. (11) by inner product:

$$\left\langle X(\mathbf{x},\xi)\Psi_k(\xi) \right\rangle = \left\langle \sum_{j=0}^{P} \alpha_j(\mathbf{x})\Psi_j(\xi), \Psi_k(\xi) \right\rangle \tag{11}$$

$\langle \bullet \rangle$ represents the inner product, which can be expressed by the following formula:

$$\langle f(\xi)g(\xi) \rangle = \int_R f(\xi)g(\xi)w(\xi)d\xi \tag{12}$$

For Gaussian random variable, the basis functions are Hermite orthogonal polynomials. Because of orthogonality, Eq. (11) can be transformed to Eq. (13)

$$\left\langle X(\mathbf{x},\xi)\Psi_k(\xi) \right\rangle = \alpha_k(\mathbf{x})\Psi_k^2(\xi) \tag{13}$$

And then it can be derived:

$$\begin{aligned} \alpha_k(\mathbf{x}) &= \frac{\left\langle X(\mathbf{x},\xi), \Psi_k(\xi) \right\rangle}{\Psi_k^2(\xi)} \\ &= \frac{1}{\Psi_k^2(\xi)} \int_R \alpha^*(\mathbf{x},\xi)\Psi_k(\xi)\omega(\xi)d\xi \end{aligned} \tag{14}$$

The sampling approaches can be divided into random sampling method and deterministic sampling method. Random sampling method uses MCS, LHS and other methods to compute the projection integrals. However, its convergence rate is low. Deterministic sampling method uses the quadrature for the numerical

evaluation of the unknown coefficients. Using *n*-dimensional Gauss-Hermite quadrature, with *q* points in each dimension, we can compute the unknown coefficients by Eq. (15):

$$\alpha_k = \frac{1}{\left\langle \Psi_k^2 \right\rangle} \sum_{i_1=1}^{q} \cdots \sum_{i_n=1}^{q} u(x_{i_1}, \cdots, x_{i_n}) \Psi_k(x_{i_1}, \cdots, x_{i_n}) \prod_{k=1}^{n} \omega_{i_k} \quad (15)$$

In Eq. (15), one-dimensional integral is expanded into a high dimensional form by tensor product, the calculation times of which require $(p+1)^n$ points for *p*-th order chaos. For low-dimensional problems, the sampling efficiency of deterministic sampling method has been greatly improved compared with random sampling method. However, the calculation times grow exponentially with the increasing dimensions.

The regression method is another approach to compute the coefficients using a linear equation system based on a selected set of points. A linear system of equation can be obtained by:

$$\boldsymbol{\alpha} \boldsymbol{\Psi}^T \boldsymbol{\Psi} \boldsymbol{\Psi}^T \boldsymbol{\alpha})^{-1} \cdot \quad ^T \cdot \quad ^* \quad (16)$$

where $\boldsymbol{\Psi}$ is given by $\boldsymbol{\Psi}_{ij} = \Psi_j(\xi^i), i = 1, \ldots, N; j = 0, \ldots, P-1$. The accuracy of regression method depends on the selection of sample points in design space. According to Ref. [12], the optimal design is given by the roots of Hermite polynomial, which the optimal sample points are $(p+1)^n$. The samples points of NIPC with projection method is $(p+1)^n$, which grows exponentially with the increasing number of input dimensions. Although the optimal design is $(p+1)^n$ for NIPC with regression method, the samples points can be reduced. The sample points are 2(P+1), which gives a better approximation at each polynomial degree. To study how the number of samples influences to the analysis results, the oversampling ratio n_p is defined as

$$n_p = \frac{number\ of\ samples}{P+1} \quad (17)$$

After computing the unknown coefficients, the approximate PCE model is built, and then the model is used to compute the first two statistical moments analytically.In order to compute the Sobol's indices, the Sobol's decomposition based on PCE should be derived. The detail derivation process is in Ref. [16].

4 Stochastic transonic aerodynamics analysis considering geometric uncertainty

4.1 The description of geometric uncertainties

In engineering, the geometric uncertainty on aerodynamic surfaces resulting from manufacturing errors or wearing is unavoidable, which has significant influence on the aerodynamic performance. Therefore, UQ and GSA considering geometric uncertainty are conducted in this section. To carry out this work, the first step is to describe the geometric uncertainty caused by manufacturing errors in the computing environment.

With a large amount of geometric statistical manufacturing error data of airfoil, the main geometric variation modes are obtained by PCA. It gets the main variation modes based on the statistical manufacturing error data, and is used to achieve the geometric variation [17-19]. The description of the geometric uncertainty of airfoil is shown in Eq. (18):

$$g = g_n + \bar{g} + \sum_{i=1}^{n_s} \sigma_i z_i v_i \quad (18)$$

where g_n is the nominal geometry; $\bar{g}$ is the average geometric variation; v_i is the geometric mode shape; n_s is the number of mode shapes used to represent the variation in geometry. The geometric mode can be computed by PCA based on a manufacturing samples. σ_i is the *i*-th singular value of the measurement snapshot matrix, which represents the geometric variability attributable of the *i*-th mode. z_i is a random parameter which obeys the standard normal distribution; thus, the product $\sigma_i z_i$ is the stochastic contribution of *i*-th mode.

It is difficult to describe this geometric variation in the computing environment. In Ref. [19], a Gaussian random process simulation is used to obtain the geometric data. Then PCA is used to obtain main geometric modes. By changing the parameter of these parametric methods, the geometric variation is realized. Generally, these parametric methods need a lot of parameters to represent the airfoil shape. To reduce the dimensions of the variables, the

PCA technology combined with airfoil parameterization is used to describe the geometric variation is used. In this paper, we use a parameterized representation of the airfoil ARE2822 by *CST* method with 24 parameters. The data of the measurement points on the airfoil surface are obtained by random perturbation of *CST* parameters. In this way, the PCA based sample data is conducted. The first 12 modes obtained by PCA are showed in Fig.3. The 12 modes include 6 modes of the upper surface (mode 2, mode 3, mode 5, mode 7, mode 9, mode 10) and 6 modes of the lower surface (mode 1, mode 4, mode 6, mode 8, mode 11, mode 12). It can be seen that the lower-order modes in these modes are global geometric deformation modes and present some typical geometric deformation. Specifically, The mode 1 and 2 are the scale modes in the thickness direction; mode 3 and mode 4 are translation modes of the maximum thickness in the axial direction; and mode 5 and 6 is the extrusion mode of the upper surface; So, the number of parameters used to describe the geometric variation is reduced to a large extent and the typical deformation modes are obtained through the PCA technique.

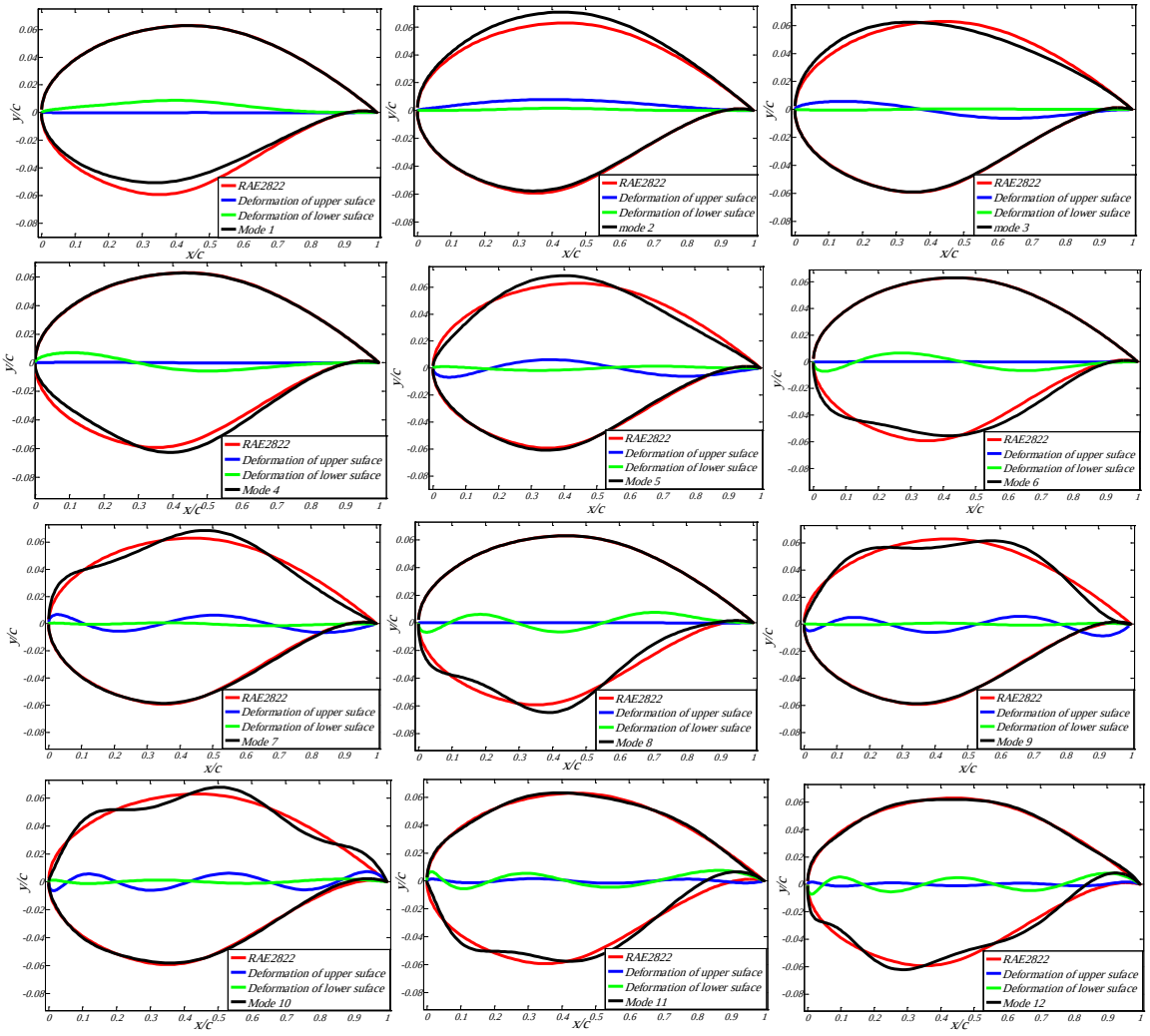

Fig.1 RAE2822 airfoil deformation of the first 12 modes

4.2Uncertainty quantification of aerodynamics

UQ of aerodynamics is conducted in the section. The uncertain variables are z_i (i=1, 2,..., 12) in Eq.(18) , which obey Gaussian distribution and are independent from each other. The flow state is selected in a transonic region (Ma=0.73, α=2.5°, Re=3.0×10 ^{6}); NIPC and MCS are used to quantify uncertainty. MCS

is used to aim at validating the accuracy and efficiency of NIPC. The computational cost of MCS is 5000. For 12 dimensional problem, If we use the NIPC with projection method, the number of samples is 531441 when polynomial chaos degree p is 2, which is unacceptable computational cost. The sample points of NIPC with regression is natively smaller than that of NIPC with projection. So, The NIPC with regression is used to UQ of aerodynamics. Fig. 2 shows the range of geometric uncertainty in the paper.

Fig.3 shows the standard deviation distribution of the pressure coefficient along the airfoil surface. It shows that the aerodynamic loads are sensitive to the geometric variation of the upper surface. In the transonic region, the location of shock fluctuates with the change of the geometric shapes, which can result in intensive fluctuations of the flow variables. We call the region in which the standard variations become much larger suddenly as shock disturbance region. Fig.4 shows the standard deviation distribution of the skin-friction coefficient along the airfoil surface. It can be seen that the skin-friction behavior displays discrepancies from the pressure coefficient. The variation of C_f is similar to that of C_p before and in the shock disturbance region. However, the difference occurs in the downstream region of the shock disturbance region; the standard deviation keeps larger magnitudes below the shock disturbance region, and then gradually decreases. This indicates that not only the shock wave but also the boundary-layer separation is sensitive to geometric uncertainty in the transonic region.

The accuracy and efficiency of NIPC is verified by the comparing the results of NIPC and MCS. The 2 order polynomial chaos are used to build PCE model, and the influence of the number of sample points on the results of UQ is studied. The number of sample points is changed by varying the parameter n_p in Eq. (17). Table 1 shows the mean value, standard deviation (*StD*) and coefficient of variation (Cov) of UQ of aerodynamic coefficients by NIPC and MCS. From Table 1, when the n_p is higher than 2, the results agree with those of the MCS; when n_p is 6, the accuracy of NIPC decreases. From Fig.3 and 4, the results of NIPC coincide well with those of MCS when n_p=4. Table 1 also displays the computational cost, which indicates that the cost of NIPC is much lower than MCS.

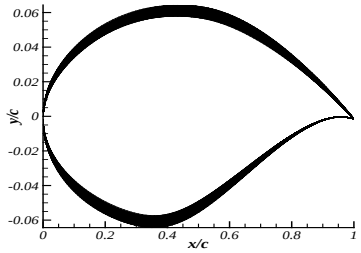

Fig. 2 The range of geometric uncertainty

Table 1. The results of UQ of aerodynamic coefficients

		NIPC				MCS
		p=2,n_p=1	p=2,n_p=2	p=2,n_p=4	p=2,n_p=6	
C_l	*Mean*	0.7216	0.7232	0.7232	0.7232	0.7237
	StD	0.0217	0.0097	0.0093	0.0085	0.0098
	Cov	0.0301	0.0134	0.0129	0.01178	0.0136
C_d	*Mean*	0.0165	0.0163	0.0163	0.0163	0.0163
	StD	0.0026	0.0013	0.0012	0.0011	0.0012
	Cov	0.1576	0.0798	0.0736	0.0675	0.0736
C_m	*Mean*	0.2715	0.272	0.2716	0.2717	0.2718
	StD	0.0057	0.0057	0.0055	0.0050	0.0055
	Cov	0.0210	0.0210	0.0203	0.0184	0.0202
L/D	*Mean*	43.914	44.627	44.629	44.6516	44.6821
	StD	9.2209	3.3608	3.1835	2.8752	3.2538
	Cov	0.2030	0.0753	0.0713	0.0644	0.0728
N		91	182	364	546	5000

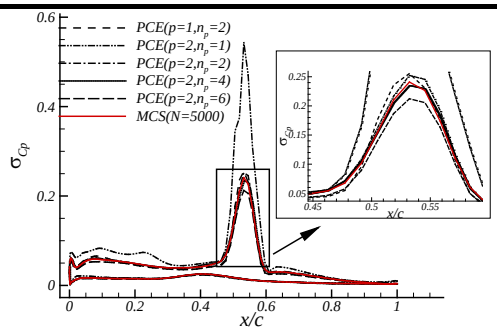

Fig. 3 Standard deviation distribution of the pressure coefficient on the airfoil surface

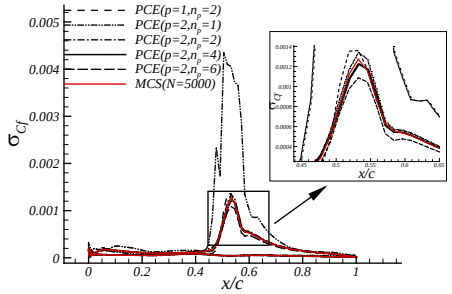

Fig. 4 Standard deviation distribution of the skin-friction coefficient on the airfoil surface

4.3 Sensitivity analysis of aerodynamics

Through GSA, we can find out important deformation modes, which provide a useful reference for subsequent design work and manufacturing process. The NIPC method (p=2, n_p=4) is used to Sobol's analysis. The aerodynamic load distribution and aerodynamic coefficients are included for Sobol's analysis. Figs.5 and 6 show the results of Sobol's analysis of the pressure and friction coefficient distribution. The partial standard deviation, total standard deviation and standard deviation caused by the coupling effect for each mode are given in Figs. 5 and 6. It can be seen that the deformation modes of the upper surface is much more important than those of lower surface to transonic aerodynamic loads(C_p and C_f). Specifically, the first 3 modes is important to aerodynamic load distribution. To C_p distribution, the main variation of the mode 2, 3 and 5 is on shock distribulence region. To C_f distribution, The main variation of mode 2 and 5 is in both shock distribulence region and boundary layer separation region; while the main variation of mode 3 is only in shock distribulence region. In addition, it can also be observed that the coupling effect among geometric deformation modes is weak in Fig.5 and 6. From Section 4.1, we can observe that mode 1 and 2 are the scale modes in the thickness direction; mode 3 and mode 4 are translation modes of the maximum thickness in the axial direction; and mode 5 is the extrusion mode of the upper surface. We can draw the following conclusions: the scale mode and extrusion mode is important to the flow characteristic of shock wave and boundary layer separation, but the translation mode is only important to flow characteristic of shock wave.

Aerodynamic coefficients including lift coefficient (C_l), drag coefficient(C_d), moment coefficient(C_m)and lift-to-drag ratio(L/D). For the C_l, the mode 1 and 2 is important, which indicate that the scale modes is important to C_l. For the C_d and L/D, the mode2,3 and 5 is important, the first 3 deformation modes of the upper surface has bigger contribution. For the C_m, The scale mode of upper surface is most important. In addition, it can also be seen that the coupling effect among deformation modes is very weak.

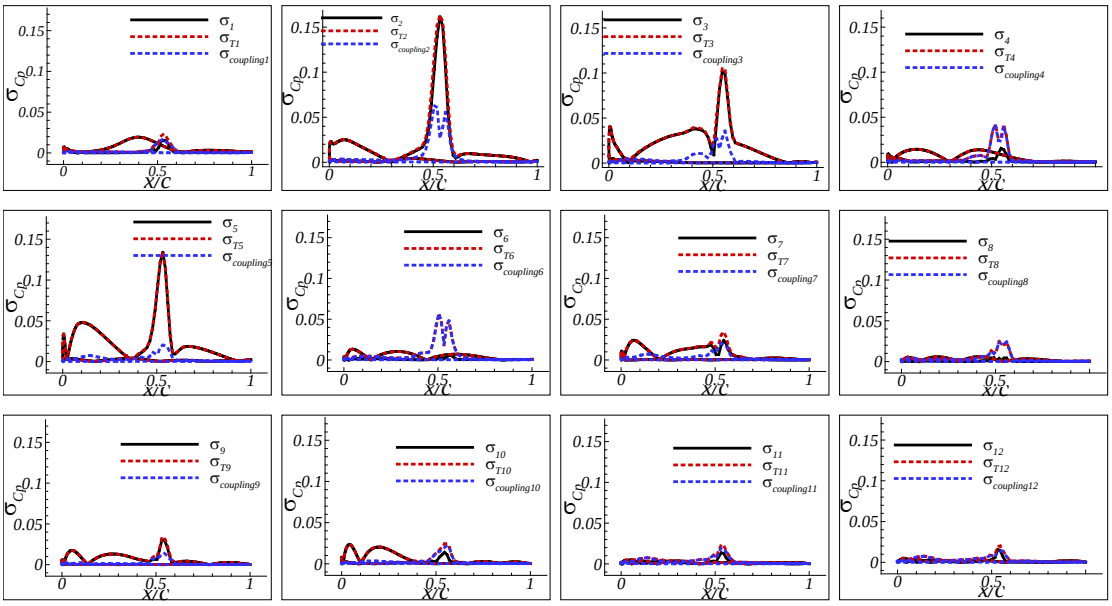

Fig.5 The results of CP distribution by Sobol's analysis (σ_i is the partial standard variation with uncertain variable i; σ_{Ti} is the total partial standard variation with uncertain variable i; $\sigma_{couplingi}$ is the nonlinear coupling effect among uncertain variable i and other uncertainty variables)

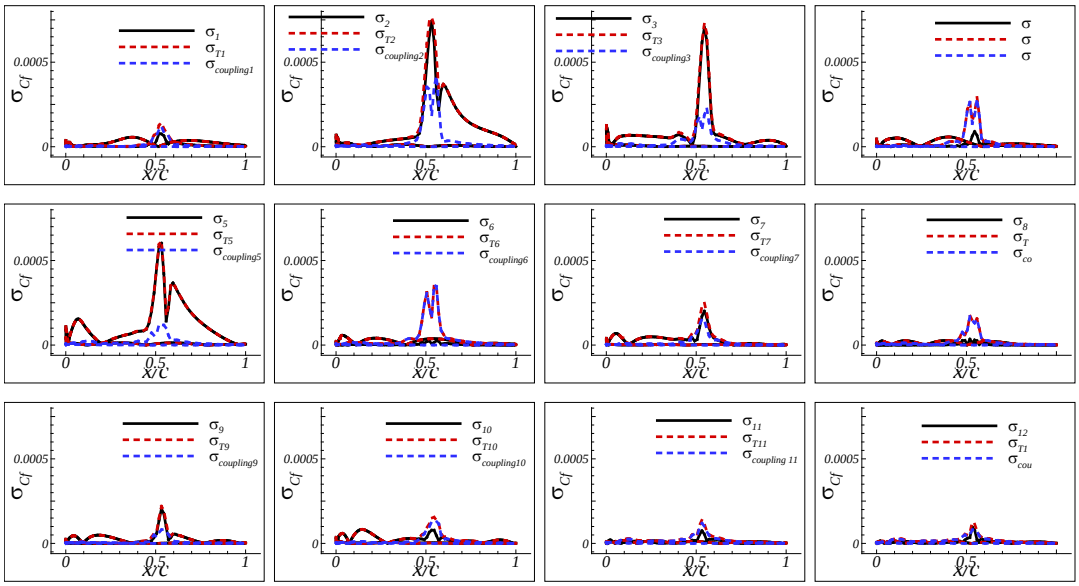

Fig.6 The results of C_f distribution by Sobol's analysis (σ_i is the partial standard variation with uncertain variable i; σ_{Ti} is the total partial standard variation with uncertain variable i; $\sigma_{couplingi}$ is the nonlinear coupling effect among uncertain variable i and other uncertainty variables)

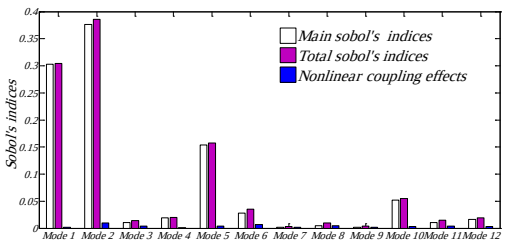

a.Sobol's indices for C_l

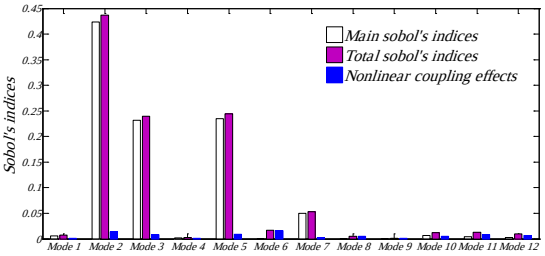

b. Sobol's indices for C_d

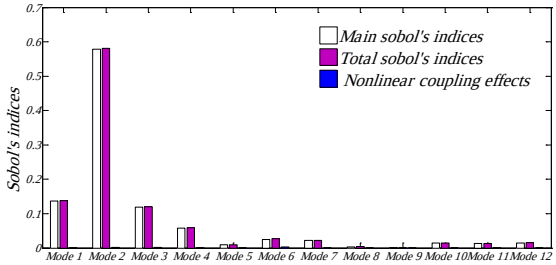

c.Sobol's indices for C_m

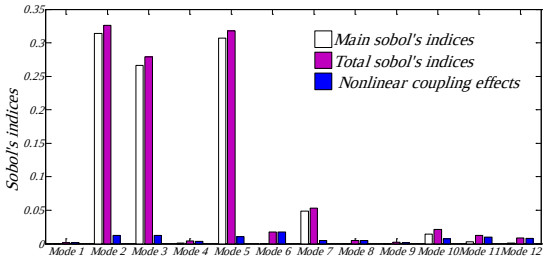

d. Sobol's indices for *L/D*

Fig.7 The results of Sobol's analysis of aerodynamics (a. Sobol's indices for C_l; b. Sobol's indices for C_d; c. Sobol's indices for C_m; d. Sobol's indices for *L/D*.)

Table 2. The comparison of the UQ results for aerodynamic coefficients between the selected 4 modes and the full 12 modes

		n=4(NIPC)	*n=12*(NIPC)
C_l	*Mean*	0.7234	0.7232
	StD	0.0096	0.0097
C_d	*Mean*	0.0163	0.0163
	StD	0.0012	0.0013
C_m	*Mean*	0.2718	0.2720
	StD	0.0053	0.0057
L/D	*Mean*	44.679	44.627
	StD	3.1699	3.3608
N		32	182

From the results of GSA, It can be observed that mode 1, 2, 3 and 5 is important to aerodynamics. So, The UQ of aerodynamics is conducted considering the 4 modes. Moreover, Because the coupling effects among the modes from the GSA, we adopt regression method with parameter p=2,n_p=2 to build the PCE model without the interaction terms to UQ. The comparison of the UQ results is showed in table 2, It can be observed that the UQ results is relatively small difference each other; and the

number of sample points are reduced from 182 to 32. That is to say, The unimportant modes are eliminated and PCE model can be modified by GSA, which can reduce the computational cost in UQ and future robust design .

5 Conclusion

In the paper, the NIPC with regression method was used to UQ and GSA for transonic aerodynamics with geometric uncertainty. From the results of UQ, the fluctuation of aerodynamic characteristics is mainly centered in the shock distrbulence region and boundary layer interference region in transonic region. The characteristics of shock wave is sensitive to geometric uncertainty, and since the transonic drag mainly includes wave drag, so the transonic drag is sensitive to geometric uncertainty. From the results of GSA of aerodynamic loads, it shows that the first three deformation modes of the upper surface have the greatest impact on the aerodynamic characteristics. Specifically, the scale mode and extrusion mode are important to the flow characteristics of shock wave and boundary layer separation, but the translation mode is only important to the flow characteristics of boundary layer separation. Moreover, from the results of GSA of aerodynamic coefficients, we can observe that the scale modes(mode 1 and 2) are important to lift characteristics while The contribution of the transition modes(mode 3 and 4) is negligible; The first 3 modes of the upper airfoil surface is important to drag and lift-to-drag characteristics. By GSA, we can eliminate unimportant geometric modes and simplify model for UQ and learn which typical modes is important to transonic aerodynamics, which is helpful for transonic airfoil design.

6 Reference

[1] Zang T A, Hemsch M J, Hilburger, M W, Kenny S P and Lucking J M et al, Needs and opportunities for uncertainty-based multidisciplinary design methods for aerospace vehicle. NASA/TM-2002-211462. Langley Research Center, 2002

[2] Yao W, Chen X Q, Luo W C, Michel V T and Guo J. Review of uncertainty-based multidisciplinary design optimization methods for aerospace vehicles. *Progress in Aerospace Sciences*, Vol.47, pp.450-479,2011.

[3] Pelletier D, Turgeon E and Lacasse D. Adaptivity, sensitivity, and uncertainty: toward standards of good practice in computational fluid dynamics. *AIAA Journal*, Vol.41, No.10, pp. 1925-1932, 2003.

[4] Luckring J M, Hemsch M J and Morrison J H. Uncertainty in computational aerodynamics. AIAA paper 2003-409, 2003.

[5] Walters R W and Huyse L. Uncertainty analysis for fluid mechanics with applications. NACA/CR-2002-211449.

[6] Mathelin L, Hussaini M Y and Zang T Z. Stochastic approaches to uncertainty quantification in CFD simulations. *Numerical Algorithms*, Vol.38, No.1, pp.209-236, 2005.

[7] Knio O M and Maitre O P L. Uncertainty propagation in CFD using polynomial chaos decomposition. *Fluid Dynamics Research*, Vol.38, pp. 616–640, 2006.

[8] Najm H N. UQ and polynomial chaos techniques in computational fluid dynamics. *Annual Review of Fluid Mechanics*, Vol.41, pp. 35–52 , 2009.

[9] Wei P F, Lu Z Z and Song J W. Variable importance analysis: A comprehensive review. *reliability engineering and system safety*,Vol142, pp. 399-432,2015.

[10] Sobol I M. Global Sensitivity Indices for Nonlinear mathematical models and their monte carlo estimates. *Mathematics and Computers in Simulation*, Vol55, pp. 271-280, 2001.

[11] Saltelli A, Ratto M and Andres T et al. Global sensitivity analysis,The Primer. England: John Wiley&Sons,Ltd, 2008.

[12] Bruno S. Global sensitivity analysis using polynomial chaos expansions. *Reliability engineering and system safety*, Vol 93, pp. 964-979,2008.

[13] Loeven G J A, Witteveen J A S and Bijl H. Probabilistic collocation: an efficient non-intrusive approach for arbitrarily distributed parametric uncertainties. AIAA-2007-317.

[14] Simon F, Guillen P, Sagaut P and Lucor D. A gPC-based approach to uncertain transonic aerodynamics. *Comput.Method Appl.Mech.Engrg*, Vol.199, 2010, pp. 1091-1099.

[15] Chasseing J C and Lucor D. Stochastic investigation of flows about airfoils at transonic speeds. *AIAA Journal*, Vol.48, No.5, pp: 918-949,2010.

[16] Hosder S and Bettis R B. Uncertainty and sensitivity analysis for reentry flows with inherent and model-form uncertainties. *Journal of spacecraft and rockets*, Vol49, No.2, pp. 193-205, 2012.

[17] Garzon V and Darmofal D. Impact of geometric variability on axial compressor performance. *Journal of Turbomachinery*, Vol.125, No.4, pp. 692-703, 2003.

[18] Thanh T B and Willcox K. Parametric reduced-order models for probabilistic analysis of unsteady aerodynamic Applications. *AIAA Journal*, Vol.46, No.10, pp 2520-2529, 2008.

[19] Chen H, Wang Q Q, Hu R and Paul C. Conditional sampling and experiment design for quantifying manufacturing error of transonic airfoil. AIAA paper 2011-658, 2011.

[20] Kulfan B M and Bussoletti J E. Fundamental parametric geometry representations for aircraft component shape. AIAA paper, pp 1-45, 2006.

10 Contact Author Email Address

wxj8905@126.com

Copyright Statement